High-power wavelength-tunable circular-grating surface-emitting distributed Bragg deflector lasers

R. S. Penner,[a] R. Bedford, H. Luo, S. Mendes, and M. Fallahi
Optical Sciences Center, University of Arizona, Tucson, Arizona 85721

(Received 30 September 1999; accepted for publication 19 January 2000)

We present a promising approach to achieve wavelength tuning in high-power circular-grating surface-emitting lasers. A transparent electrode of indium tin oxide (ITO) was used to inject carriers into the second-order grating section of the device. Powers in excess of 225 mW and slope efficiencies of better than 0.40 mW/mA are reported. A continuous tuning range of 0.5 nm was achieved, while an overall wavelength shift of 1 nm was obtained for an ITO injection current of 30 mA. © *2000 American Institute of Physics.* [S0003-6951(00)03511-7]

Wavelength tunability is of great importance in optical communication and spectroscopy applications. Circular-grating surface-emitting lasers (CGSELs) provide both high output power and the added benefit of implementing arrays of such devices. The ability to dynamically control the wavelength of individual lasers is tremendously beneficial.

Over the past decade there has been considerable interest in CGSELs. Beginning with the theoretical discussions[1] and the demonstration of the first electrically pumped device in 1992,[2] CGSELs have improved in both performance[3] and functionality.[4] In this letter, we report dynamic wavelength tuning of high-power circular-grating surface-emitting lasers. A concentric second-order circular grating provides both feedback and surface outcoupling. An indium–tin–oxide (ITO) annular region, covering the grating, was used as a low-loss transparent electrode and enabled wavelength tuning without the need for epitaxial regrowth.

Grating-based outcoupling allows enormous flexibility in device design. Surface outcoupling perpendicular to the plane (first-order diffraction) can be achieved with a second-order grating. Additionally, this configuration also satisfies the Bragg condition for feedback. Thermally induced shifts in lasing wavelength are well documented.[5] The advantage of the procedure that we have adopted is that a localized thermal effect and a carrier-injection effect are realized. Therefore, tuning of individual devices within an array is possible. Thermal effects are realized through both the thermal coefficient of the refractive index, $\beta(T,\lambda)=dn/dT$, and the coefficient of thermal expansion, $\alpha(T)$. The change in grating periodicity resulting from changes in temperature is given in Eq. (1), where Λ denotes the initial grating period,

$$\Delta\Lambda(T)=\alpha(T)^{*}\Lambda^{*}\Delta T. \quad (1)$$

However, given that at room temperature $\beta\approx 3\times 10^{-4}\,^{\circ}\mathrm{C}^{-1}$ and $\alpha\approx 6.8\times 10^{-6}\,^{\circ}\mathrm{C}^{-1}$ for bulk GaAs,[6] the relative contribution of the shift in periodicity is not significant. As a consequence of the positive value of β, increases in temperature cause an increase in the refractive index and, therefore, a redshift of the emission wavelength. The change in effective index due to carrier injection has been investigated by a number of groups for both optical and electrical carrier injection.[7] Three main effects result from carrier injection: bandfilling, band-gap shrinkage and free-carrier absorption. For differing carrier concentrations and wavelengths of interest, a particular regime dominates. The magnitude and sign of the shift in effective index of refraction is correspondingly dependent on the given carrier effect.

A strained triple-quantum-well graded-index separate-confinement heterostructure (GRINSCH) structure was used for these devices. The epitaxial layers were grown on an n^{+} GaAs substrate using molecular-beam epitaxy. A 150 Å GaAs etch-stop layer was incorporated into the growth structure at a position 0.3 μm above the quantum wells. The etch stop served to accurately position the gratings for optimal coupling. The Be-doped p layer extended both above and below the etch-stop layer. This doping structure prevented recombination in the etch stop, provided a high doping level for the current injection through the ITO, and produced a low-threshold device.[8] The Ti–Pt–Au p contacts, consisting of 100-μm-diam circles, were created using a lift-off process. Contact mesas were defined by electron–cyclotron-coupled reactive-ion etching (ECR-RIE) using a chlorine/methane mixture and were selectively etched down to the stop layer with a hot BOE:HF solution. Second-order concentric circular gratings were patterned in a ZEP-520 resist using a JEOL-6400 scanning electron microscope (SEM) equipped with nanometer pattern generation system. The gratings were then etched to a depth of about 0.12 μm using ECR-RIE. Ni–Ge–Au n contacts were used. A 200-nm-thick ITO film was deposited onto the sample using rf sputtering. The ITO was subsequently patterned and etched in HCl to produce annular regions of ITO. The first 10 μm of the grating was bare of ITO in order to provide electrical isolation between the ITO and the p-contact mesa. The devices were then annealed at 415 °C using a rapid thermal process. Prior analysis of the electrical properties of ITO conducted by our group revealed that a minimum serial resistance of approximately 100 Ω is achieved for annealing times and temperatures comparable to those used for the n and p contacts. Therefore, a single annealing process was used. A SEM micrograph of the grating/ITO cross section and a schematic of the laser are shown in Fig. 1.

The lasers were tested at room temperature under pulsed

[a]Electronic mail: penner@optics.arizona.edu

 © 2000 American Institute of Physics
Downloaded 05 Apr 2004 to 128.196.114.77. Redistribution subject to AIP license or copyright, see http://apl.aip.org/apl/copyright.jsp

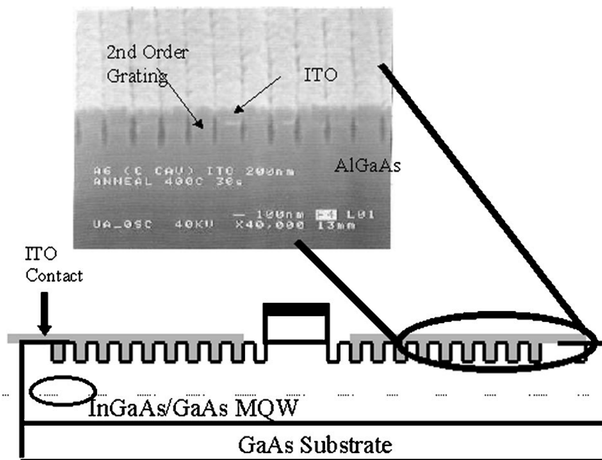

FIG. 1. Cross section of circular-grating surface-emitting laser with ITO.

operation. A plot of the output power versus injection current is given in Fig. 2. A threshold current of 28.5 mA (threshold current density of 363 A/cm^2) was confirmed using an optical spectrum analyzer. Linear regression of the data provides a slope efficiency of 0.43 mW/mA, which corresponds to an external differential quantum efficiency of 34%, which was maintained over the whole operating current range. An output power in excess of 220 mW was obtained. The characterization of wavelength tuning was performed at 350 mA ($\sim 12\ I_{th}$), which corresponded to an output power of over 110 mW. The near- and far-field irradiance distributions are shown in Fig. 3. The distributions are characteristic of the $m=1$ mode.

ITO injection was achieved with the probe contact near the outer annulus of the grating (Fig. 1). Upon two-probe testing of the ITO, there was little difference in contact resistance for probes located at different positions on the grating. Direct current ITO injection currents up to 30 mA were used. Considering the area of grating to be 0.12 mm^2, and assuming uniform injection, this corresponds to ITO injection current densities on the order of 25 A/cm^2. Forward- and reverse-biased ITO currents were investigated; however, the best results were obtained under reverse bias. Figure 4 shows the wavelength tuning that was achieved for a reversed-bias injection. As shown in Fig. 4, a 1 nm tuning range was accomplished. The initial lasing wavelength was 982 nm. The plot is broken to indicate the mode hopping which occurred as the ITO injection current was increased from 15 to 20 mA. The trend lines for the two portions of the reverse-bias plot clearly suggest that the peak emission wavelength has jumped longitudinal modes as was observed on the spectrum analyzer. As the far field did not change with ITO injection, this confirms our suspicion that the change in mode was not a transverse mode. The fact that both forward and reverse biasing results in a redshift in the wavelength (positive $\Delta\lambda$) suggests that localized thermal effects dominate. However, carrier injection does contribute to the change in refractive index, and therefore lasing wavelength, as evidenced by the difference in the amount of wavelength tuning for a given current under forward- or reverse-biased conditions. Since the ITO is responsible for both thermal and carrier effects, optimization of its properties are important. Optical absorption and electrical resistance must be minimized. As a result, carrier effects should have a greater contribution

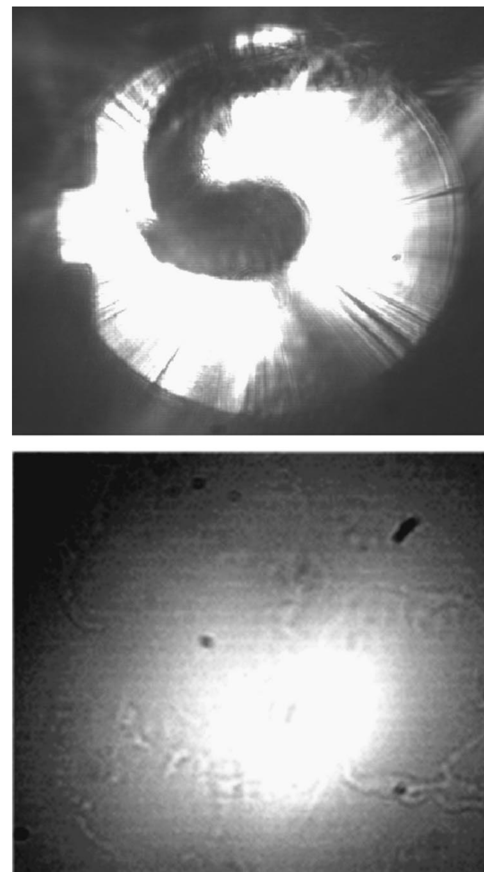

FIG. 3. Near- and far-field irradiance.

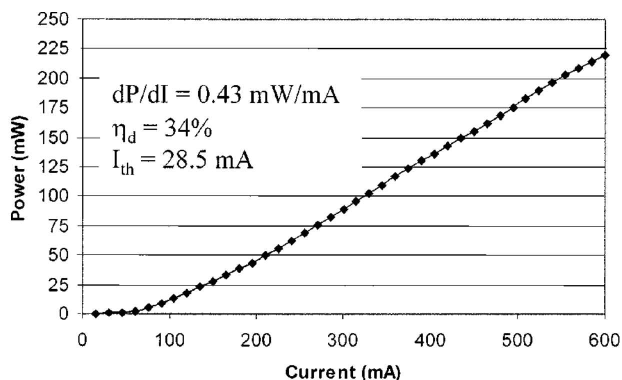

FIG. 2. Output power vs injection current for high-power circular-grating surface-emitting laser.

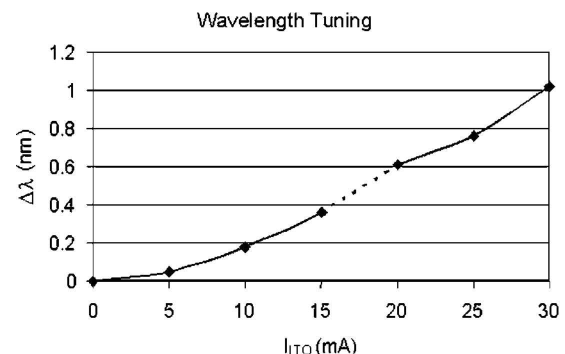

FIG. 4. Wavelength shift vs ITO injection current.

Downloaded 05 Apr 2004 to 128.196.114.77. Redistribution subject to AIP license or copyright, see http://apl.aip.org/apl/copyright.jsp

to the wavelength tuning process. This is a desirable goal given the faster tuning speed associated with carrier dynamics as opposed to thermal effects.

We have demonstrated the ability to dynamically shift the output wavelength through the injection of current into ITO. A shift of 1.0 nm for an ITO injection current of 30 mA was observed for a device operating at 110 mW output power.

This work was supported by DARPA/AFOSR.

[1] M. Toda, IEEE J. Quantum Electron. **26**, 473 (1990).
[2] C. Wu, M. Svilans, M. Fallahi, I. Templeton, T. Makino, J. Glinski, R. Maciejko, S. Najafi, C. Maritan, C. Blaauw, and G. Knight, Electron. Lett. **28**, 1037 (1992).
[3] M. Fallahi, M. Dion, Z. Wasilewski, M. Buchanan, M. Nournia, J. Stapledon, and R. Barber, Electron. Lett. **31**, 1581 (1995).
[4] S. Kristjansson, M. Li, N. Eriksson, M. Hagberg, K. Killius, and A. Larsson, IEEE Photonics Technol. Lett. **9**, 416 (1997).
[5] G. Agrawal and N. Dutta, *Semiconductor Lasers*, 2nd ed. (Van Nostrand Reinhold, New York, 1993).
[6] S. Adachi, *GaAs and Related Materials Bulk Semiconducting and Superlattice Properties* (World Scientific, Singapore, 1994).
[7] B. Bennett, R. Soref, and J. Del Alamo, IEEE J. Quantum Electron. **26**, 113 (1990).
[8] M. Dion, P. Levesque, Z. R. Wasilewski, M. Fallahi, F. Chatenoud, R. L. Williams, and S. J. Rolfe, Proc. SPIE **2683**, 8 (1996).

Downloaded 05 Apr 2004 to 128.196.114.77. Redistribution subject to AIP license or copyright, see http://apl.aip.org/apl/copyright.jsp